Human motions analysis and simulation based on a general criterion of stability

Z. QIU*†‡ A. ESCANDE‡ A. MICAELLI‡ and T. ROBERT†

† Université de Lyon, Ifsttar, UMR_T9406, LBMC, Université Lyon 1;

‡ CEA LIST, Interactive Simulation Laboratory, 18, route du Panorama, BP6, FONTENAY AUX ROSES, F- 92265 France

** Corresponding author: zhaopeng.qiu@ifsttar.fr / zhaopeng.qiu@cea.fr*

Phone: 33-6-27808219

Abstract

In this paper we present a new methodology for dynamic movement planning of digital human models in constrained environments. The goal is to compute a smooth trajectory of centre of mass (CoM) that satisfies dynamic constraints throughout the whole motion. Firstly, we adapt a newly proposed dynamic stability criterion in order to define stability constraints in this work. This criterion is then used to analyze human motions from the viewpoint of stability. Then we apply the approach to compute trajectories of CoM by implementing parametric splines and optimization methods with dynamic constraints. Finally we apply the generated trajectory in a whole-body simulation in order to demonstrate the viability of this approach.

Keywords: Stability, Motion simulation, Posture and motion, Digital Human Model.

1. Introduction and related works

A digital human model (DHM) is a complex human-like system with numerous degrees of freedom. To realize DHM's interactive human-like motion is an important research problem with broad applications in many domains such as ergonomics, computer graphics, robotics, movies, games, etc. It's always hoped that the DHM can spontaneously realize human-like motions adapting to variations of environment. To achieve this goal, it's necessary to use a dynamic model instead of a kinematic model for the DHM. This brings dynamic requirements for the motions, especially the stability requirement. In this work, we use a general stability criterion to analyze the real human motions, aiming to comprehend the influence of the human/environment interactions over the balance of the human. This work can then help planning and simulating DHM's motions.

Nowadays, most realistic motions are realized with the help of motion capture (Mocap) techniques, since they can record and reproduce detailed human motions. But the Mocap suffers important limitations since it doesn't take into account the dynamics of DHMs. Dynamics based motions with controllers and planners attract more and more attention. But planning the whole-body motion is a rather time-consuming work, requiring usually several hours of computation. In this work, we propose an intermediate solution in the following steps:

- key postures definition according to the tasks and the environment;
- trajectory planning based on a simplified dynamic model;
- trajectory tracking with the help of a local dynamic controller.

Currently, we still depend on the Mocap database. In the first step, instead of computing the key postures, we extract and take advantage of the key frames in the recorded motions.

1.1. Stability

The issue of stability has been studied for many years in robotics. For a mechanical system to remain in static balance, the classic criterion is defined as: the projection of centre of mass (CoM) onto a horizontal plan should lie inside a convex support region (Wieber 2002, Bretl and Lall 2008). When the system is moving, the classic criterion is to confine the ZMP (zero moment point) or the CoP (centre of pressure) inside the supporting polygon (Sardain and Bessonnet 2004). The "projection of CoM" criterion can only treat the static cases, making it invalid in dynamic situations. The limit of the ZMP criterion is that it can only be used in

*Corresponding author. Email: zhaopeng.qiu@ifsttar.fr / zhaopeng.qiu@cea.fr

the case when the human model has co-planar contacts with the environment. To respond to this limitation, several more universal criteria are proposed: GZMP (Harada et al. 2003); the admissible wrench space and the notion of residual ball radius to evaluate the quality of equilibrium (Barthelemy and Bidaud 2008); the admissible perturbation space (Garsault 2008). The methodology we propose in this paper is based on a slight extension of the criterion developed by Garsault.

1.2. Motion simulation and animation

There are now several main techniques to simulate human motions which can generally be classified into kinematics methods and dynamics methods. The kinematics methods, mostly based on motion capture technique, can realize rather complicated and detailed human motions. But it is difficult to replay a motion if the environment or the dimensions of the human model differ significantly from those of the reference motion. Dynamics based methods, originally developed and used in robotics, are paid more and more attention thanks to their better interaction with the environment. These methods are based on the dynamic models and use control techniques to actuate the muscle forces or joints torques (Khatib et al. 2004, Collette et al. 2007). Up to now, the digital human can realize simple manipulations and locomotions by using the local controllers. When the environment or the task becomes more complex, global planners are used to plan whole-body motions by taking into account all the bodies and joints, which takes a high cost of computing time because of the high dimensionality of the configuration space. Some researchers focus their efforts in combining the two kinds of methods, by using dynamics to edit captured motions (Komura et al. 2004, Zordan et al. 2005).

1.3. Our works

Motions performed by volunteer subjects were captured, reconstructed and analyzed to extract key frames.

Based on a simplified model, we formulate the admissible perturbation space criterion. From this criterion a margin of stability is estimated and used to analyze the stability of the recorded motions.

By using the minimum experimental information (namely the state of the DHM's center of mass at key frames) and the dynamic stability constraints, we proposed a method to compute a trajectory of CoM that is smooth and dynamically stable. An example of comparison between the simulated and measured trajectory of the CoM is provided.

The viability of this approach is eventually demonstrated by the simulation of a whole-body DHM movement. The generated trajectory is tracked by a dynamic controller which successfully guided the DHM to realize a dynamic motion.

2. Materials and Methods

2.1. Data collection

In this study, motions of volunteer subjects passing under beams were recorded by virtue of a motion capture system.

A kinematic model (26 segments – 62 degrees of freedom), based on the commercial DHM Ramsis, was tailored to subject's body. Inertia Parameters were estimated from regressions (Dumas et al. 2007).

Motions were then reconstructed and analyzed by using the software RPx (Monnier et al. 2008). Trajectory, velocity and acceleration of the whole body CoM were estimated from individual segment kinematics and numerical derivation associated to low pass filtering (Butterwoth recursive 2nd order low pass filter with cut-off frequency set at 5 Hz). Motion key frames were defined by detecting the variations of the human/environment interaction (contact and grasp).

2.2. Mathematic background

a. Polytope representations and projection

In elementary geometry, a polytope is a geometric object with facets, edges and vertices, which exists in any general number of dimensions. It can be expressed in either the vertex representation (V-representation):

$$F = conv(V = \{v_1 \in \Re^n, \cdots, v_{N_v} \in \Re^n\}) = \left\{ f \in \Re^n \middle| \; f = \sum_{i=1}^{N_v} \alpha_i v_i, 0 \le \alpha_i \le 1, \sum_{i=1}^{N_v} \alpha_i = 1 \right\}$$

or half-space representation (H-representation):

$$F = \left\{ f \in \Re^n : Af \le b \; with \; A \in \Re^{m \times n}, b \in \Re^m \right\}.$$

Given a set $Q \in \Re^{n_Q}$ and a set $P \in \Re^{n_P}$ with $n_Q \le n_P < \infty$, the projection of P onto Q is defined as:

$$proj_Q(P) := \left\{ q \in Q \middle| \; \exists p \in P \; with \; q = M_p p + m_0 \right\}$$

for some given $M_p \in \Re^{n_Q \times n_P}$ and $m_0 \in \Re^{n_Q}$.

Theorem: If $P \in \Re^d \times \Re^k$ is a polytope, then the projection of P onto $\Re^d$ is a polytope (Jones et al. 2004).

b. Skew-symmetric matrix

Les's define $z = \begin{bmatrix} z_1 \\ z_2 \\ z_3 \end{bmatrix}$ and its skew-symmetric matrix $\hat{z} = \begin{bmatrix} 0 & -z_3 & z_2 \\ z_3 & 0 & -z_1 \\ -z_2 & z_1 & 0 \end{bmatrix}$, the cross product of z and any $x \in \Re^3$ can be calculated by

$$z \wedge x = \hat{z}\, x .$$

2.3. The stability criterion formulation

We explore our criterion using a simplified model (see Fig. 1). It has a point mass with its position defined as $x \in \Re^3$.

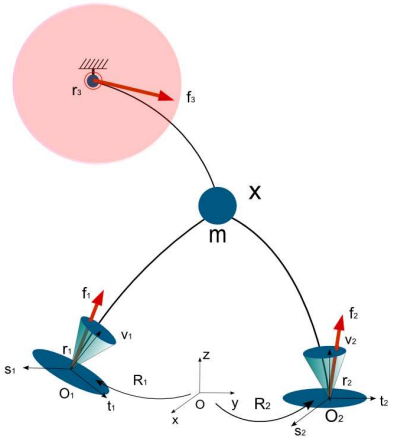

Figure 1: A simplified model for dynamic stability analysis: a point mass with two non-coplanar contacts and one grasp.

An exterior force (a contact or a grasp) is expressed by a vector $f_i = \begin{bmatrix} f_{xi} & f_{yi} & f_{zi} \end{bmatrix}^t \in \Re^3$. It is applied on the point $r_i \in \Re^3$. The gravity is applied on the point mass: $g = \begin{bmatrix} 0 & 0 & -9.81 \end{bmatrix}^t \in \Re^3$. All variables are expressed in the global coordinate system (GCS). We attach a local coordinate system (LCS) at the point of contact whose three axis are respectively (expressed in the GCS): the normal direction v_i, the sagittal direction s_i and the tangent direction t_i. Suppose that this LCS has a rotation R_i regarding the GCS which defines les relations:

$$v_i = R_i \begin{bmatrix} 0 \\ 0 \\ 1 \end{bmatrix},\ s_i = R_i \begin{bmatrix} 1 \\ 0 \\ 0 \end{bmatrix} \text{ and } t_i = R_i \begin{bmatrix} 0 \\ 1 \\ 0 \end{bmatrix}.$$

The dynamic equations of the system:

$$m\ddot{x} - mg = \sum_{i=1}^{n+k} f_i \qquad (1)$$

$$\hat{x}\, m\ddot{x} = \sum_{i=1}^{n+k} (\hat{r}_i\ f_i) + \hat{x}\, mg \qquad (2)$$

Denote a vector $f \in \Re^{3(n+k)}$ integrating the n forces of contact and the k grasping forces, the dynamic term is regarded as a perturbation applied on the system:

$$w = m\ddot{x} - mg \qquad (3)$$

Then, the equations (1) and (2) can be expressed as:

$$w = Af + b \qquad (4)$$

$$\hat{x}\, w = Cf + d \qquad (5)$$

where $A = [I, \cdots, I]$, $C = [\hat{r}_1, \cdots, \hat{r}_{n+k}]$ and $b = d = \begin{bmatrix} 0 & 0 & 0 \end{bmatrix}^t$.

Combining the equations (4) and (5):

$$\begin{bmatrix} I \\ \hat{x} \end{bmatrix} w = \begin{bmatrix} A \\ C \end{bmatrix} f \qquad (6)$$

For a point of contact, the condition of no-slipping is ensured by:

$$\left\| \begin{matrix} s_i^t f_i \\ t_i^t f_i \end{matrix} \right\| \le \mu_i v_i^t f_i \qquad (7)$$

The equation (7) defines the frictional cone (Coulomb Model). To simplify the problem, we only check this condition in the sagittal direction and the tangent direction:

$$\left| s_i^t f_i \right| \le \mu_i v_i^t f_i$$

$$\left| t_i^t f_i \right| \le \mu_i v_i^t f_i$$

Then the no-slipping condition can be expressed as:

$$\beta_i f_i \le 0 \qquad (8)$$

where $\beta_i = -\begin{bmatrix} \mu_i v_i^t + s_i^t \\ \mu_i v_i^t - s_i^t \\ \mu_i v_i^t + t_i^t \\ \mu_i v_i^t - t_i^t \end{bmatrix}$.

To avoid grasp breaking, a grasping force is proved to be confined by (see Appendix 1):

$$A_{gi} f_i \le b_{gi} \qquad (9)$$

The exterior forces vector f is proved to be limited by a linear inequality (see Appendix 1):

$$A_{cg} f \le b_{cg} \qquad (10)$$

Equation (10) defines a polytope in the exterior wrench space namely:

$$F = \left\{ f \in \Re^{3(n+k)} \middle| A_{cg} f \le b_{cg} \right\}$$

The equation (6) defines the projection of F onto a 6D-space which is also a polytope (see Appendix 2):

$$\mathrm{P} = \begin{bmatrix} A \\ C \end{bmatrix} F := \left\{ y = \begin{bmatrix} w \\ \hat{x}\, w \end{bmatrix} \in \Re^6 \middle|\ Hy \le h \right\}$$

Let's denote $H_1 = H(:,1:3)$ and $H_2 = H(:,4:6)$, the polytope of the admissible dynamic perturbation is expressed as:

$$\varpi := \left\{ w \in \Re^3 \middle|\ H(x)w \le h \right\}.$$

where $H(x) = H_1 + H_2\hat{x}$, then the stability criterion is :

$$\textit{The movement is stable} \Leftrightarrow H(x)w \leq h$$

This criterion is in form of a linear matrix inequality of w for a given position x.

2.4. Margin of stability

The stability criterion proposed in section 2.3 is used to analyze the margin of stability by calculating the smallest distance of the dynamic term w from the boundary of the polytope ϖ.

This distance is estimated by the "residual ball radius", i.e. the radius of the largest hypersphere centered in w included in the polytope ϖ (Barthelemy and Bidaud 2008).

In this study the foot-ground interaction is modelled by four contact points fixed in the foot segment, with unilaterality and friction constraints (μ=1.0). The hand-beam interaction is represented as a simple contact point, fixed in the hand segment, with a maximal grasping force set at 600N.

2.5. Trajectory generation

We generate the 3D trajectory of CoM by computing optimized discrete B-splines. The advantage of a B-spline is the possibility to manipulate the local curve properties as well as its derivative curves by configuring the same set of control points. We can impose conditions, for example, the positions at some frames, initial and final velocities and accelerations, and the respect of the stability criterion to guaranty the dynamic stability of the trajectory.

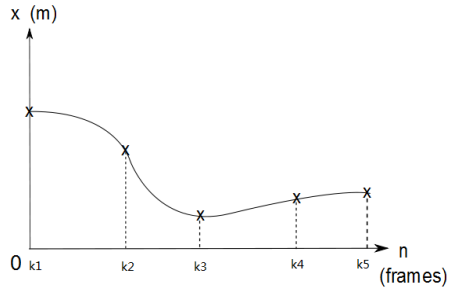

Figure 2: An example of a spline for x-direction with positions imposed at key frames. n is the number of frames. ki is the i-th key frame.

We suppose that the trajectory $p(t)$ consists of three B-splines ($x(t), y(t)$ and $z(t)$) who share the same knots and have the same number of control points. The splines are discretized by a sampling time $T = 0.01s$ which is the same as in the Mocap experiments. To represent a motion with l frames, we can note the position of the CoM at time jT as: $p(jT)$ with $0 \leq j < l$.

In the computation of trajectory, the optimization problem is formulated as follows:

Variable to optimize: Vector of control points for the three B-splines:

$$a = \begin{bmatrix} a_x{}^t & a_y{}^t & a_z{}^t \end{bmatrix}^t;$$

Objective:

- Minimize the jerk and minimize the velocity:

$$obj = min\left(\sum_{j=0}^{l} [\ddot{p}(j,a)^t Q_j \ddot{p}(j,a) + \dot{p}(j,a)^t Q_v \dot{p}(j,a)]\right)$$

where $\dot{p}(j,a)$ and $\ddot{p}(j,a)$ are respectively the velocity and the jerk at time jT in function of the control points vector a; Q_j and Q_v are the weighting matrix;

Constraints:

- Positions at key frames: $p(k,a) = p(kT)$

where $p(kT)$ is the position in key frame k of a motion;

- Zero velocities at the beginning and the end of the movement : $\dot{p}(0,a) = \dot{p}(l-1,a) = [0\ 0\ 0]^t$
- Dynamic constraints at key frames:

$$[H_1 + H_2\hat{p}(k,a)](m\ddot{p}(k,a) - mg) \leq h$$

with $\ddot{p}(j,a)$ the acceleration at time jT in function of the control points vector a.

The dimension of the vector a should be chosen to be superior to the number of imposed equality constraints, thus the optimization has enough liberties to find the optimal solution.

During the optimization and in order to save computation time, we evaluate the criterion at key frames, and verify a posteriori that it is satisfied along the whole trajectory. If not, we add key frames and launch a new optimization from previous solution.

2.6. Whole-body motion simulation

We use a dynamic controller (Collette 2009) to actuate the DHM's whole-body motion. This controller uses the generated trajectory of CoM as reference and computes the torques for the joints by Quadratic Programming (QP) optimization. The CoM tracking, hand grasping and foot placement are defined in the controller as different tasks, which are represented as objectives in the optimization. Dynamic equations, joints limits and torque limits add constraints to the optimization. It's crucial that the reference trajectory should be feasible so that the controller can find the solution.

3. Results

3.1. Motion reconstruction and analysis

The recorded motions were successfully reconstructed and accordingly we got trajectories, velocities and accelerations of the CoM, the hands and the feet. Further analyses were performed on one of these motions, displayed in Figure 3 below. The corresponding subject's stature and beam height are 1.75 m and 1.3 m respectively. In this motion, 9 key frames were identified namely:

- Starting frame
- Left foot lift-off
- Left foot landing
- Right Foot lift-off
- Hand grasp
- Right Foot landing
- Left foot lift-off
- Left foot landing
- End frame

Figure 3: Snapshots of a reconstructed motion: passing under a beam (not represented) with left hand grasp.

3.2. Motion analysis

The state of the CoM estimated from the reconstructed motion is used to compute the admissible perturbation space and the margin of stability.

The Figure 4 shows an example of the admissible perturbation space calculated around the key frame 158 in which the left foot is lifted. We can notice that the volume of polytope decreases greatly because of the lift of the left foot. This decrease occurs in x-direction, since the two feet are located initially along this direction. Due to this decrease, the dynamic perturbation term w becomes very near to the boundary of the polytope, meaning that the human takes a much larger risk of losing balance.

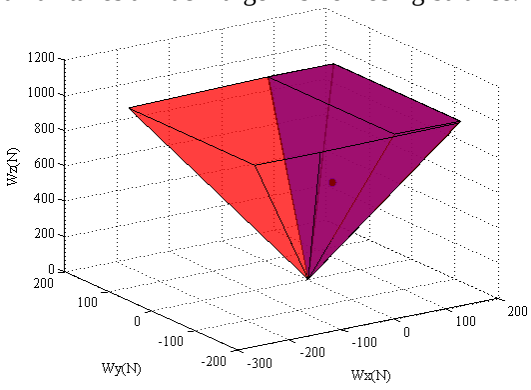

Figure 4: Two polytopes of the admissible perturbation: before (red) and after (purple) the lift of left foot (at 1.58s). The purple polytope is inside the red one. The solid point is the dynamic perturbation vector w.

The margins of stability in all the frames have been plotted in Figure 5. We can notice the discontinuities at the key frames, since the change of human/environment interactions occurs in these frames. The lift of the left foot at 1.58s brings a great risk of losing balance, causing the margin of stability fall nearly to zero. The hand grasp at 2.4s enhances significantly the safety of stability.

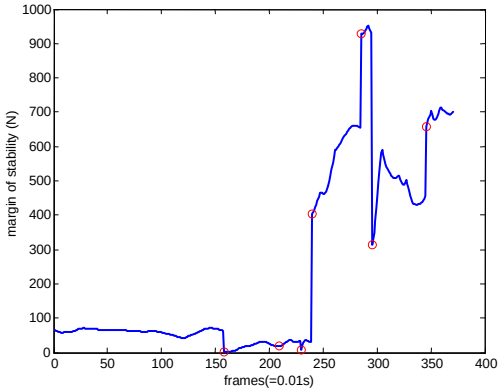

Figure 5: Evolution of margin of stability. Red circles indicate the key frames (the first and the last frames are also key frames which are not indicated in the figure).

3.3. Trajectory generation

The reconstructed positions of the CoM at the 9 key frames were used as constraints to compute a smooth and stable CoM trajectory.

The generated trajectory as well as its velocity were then compared to their counterparts in the real motion (see Figure 6 and 7).

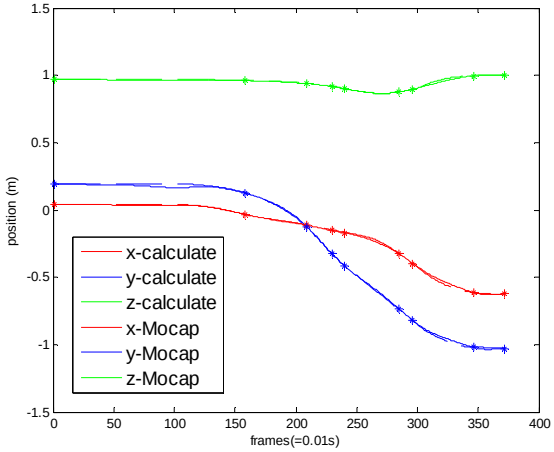

Figure 6: Comparison of the Mocap trajectory and the generated trajectory: positions expressed in three directions. * indicates the key frames in which the positions are imposed in the splines.

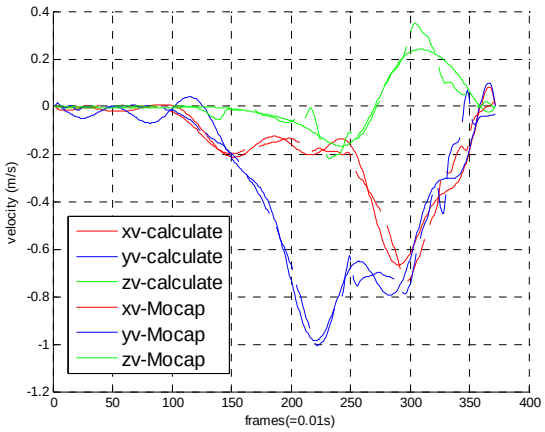

Figure 7: Comparison of the Mocap trajectory and the generated trajectory: curves of velocity.

An a posteriori checking confirmed that the stability criterion was respected at all frames. Moreover, one can remark the good fit between the experimental and simulated trajectories.

3.4. Whole-body simulation

In order to illustrate the possible use of the smooth and stable CoM trajectory, an example of dynamic whole body motion simulation based on this trajectory is presented here.

This work is carried out using the software XDE-DSIMI[1], in which a dynamic controller is coupled to a 39 degrees of freedom DHM. The dynamic controller estimates the joint torques necessary to track the CoM trajectory obtained in the previous section.

Inputting only the trajectory of the CoM leads to an overly underconstrained problem. The resulting motion is thus likely to be far from satisfying. Therefore for this study we chose to add additional task to the controller to better constrained the solution. These tasks consists in tracking trajectories of the head and polynomial interpolations for the left hand and the feet.

Figure 8 displays the simulated motion. Although this motion still needs improvements in terms of realism and naturalness, it is important to remark that the manikin keeps balance at all time. It thus validates our approach in the aspect of stability.

Figure 8: Clips of the whole-body motion in the simulation.

4. Discussion and conclusion

The dynamic stability criterion confines the dynamics of the system inside an admissible polytope to avoid slipping at contact points, grasp breaking and losing stability. The minimum distance from the dynamics vector to the boundary of this polytope is used to evaluate the margin of stability. In this work, we use this criterion for the analysis of a recorded motion. By tracing and comparing the evolutions of the margin of stability, we can evaluate the risk of losing balance in each frame. We can also see the influence of variations of contacts and grasps over the margin of stability.

An approach is proposed to plan the dynamic motion of a DHM in constrained environments. In this approach, we carry out an optimization of control points of B-splines by imposing positions and the stability constraints at key frames. In addition, objectives like minimizing jerks and velocities are used in order to make the motion more smooth and natural. In the section 3.3, we present the result of this approach to generate the trajectory of CoM for a "passing under a beam" motion.

This approach is validated by our simulation. The human model realizes the stable whole-body motion by tracking the trajectory calculated in our approach.

[1] *XDE-DSIMI ("eXtended Dynamic Engine - Distributed SIMulation Interface") is the software developed by CEA LIST for interactive simulations.

The dynamic stability criterion that we use in this study is limited by the simplification and the hypothesis in its formulation. It will be interesting in the future work to add inertia to the system and to model exterior torques at the contact and grasping points.

Our approach still start from some motion capture data: feet placement, hand grasp positions, time partition among transitions, etc. In the future, we intend to add simple planning methods and timing considerations into this approach in order to no longer depend on the motion capture database.

Acknowledgement

This study is part of the Phd thesis co-financed by two laboratories: LSI of CEA LIST and LBMC of Ifsttar. The authors would like to thank the two laboratories as well as all the colleagues for their supports and generous help to this work.

References

Barthelemy S, and Bidaud P, 2008. Stability measure of postural dynamic equilibrium based on residual radius. In 11th International Symposium of Advances in Robot Kinematics (ARK'08).

Bretl T, Lall. S, 2008. Testing static equilibrium for legged robots. IEEE Transactions on Robotics 24(4), 794-807.

Collette C, 2009. Commande dynamique d'humains virtuels: équilibre robuste et gestion de tâches. Phd thesis, UMPC Paris 6.

Collette C, Micaelli A, Andriot C, and Lemerle P, 2007. Dynamic balance control of humanoids for multiple grasps and non coplanar frictional contacts. Humanoids 2007.

Dumas R, Cheze L, Verriest J-P, 2007. Adjustments to McConville et al. and Young et al. body segment inertial parameters. Journal of Biomechanics 40, 543–553.

Garsault S, 2008. Non-gaited dynamic motion with multi-contact transition. Traineeship report, Ecole Mine de Paris.

Harada K, Kajita S, Kaneko K, and Hirukawa H, 2003. ZMP Analysis for Arm/Leg Coordination. Proc.of IEEE/RSJ Int. Conf. on Intelligent Robots and Systems.

Jones C, Kerrigan E, and Maciejowski J, 2004. Equality set projection: a new algorithm for the projection of polytopes in halfspace representation. Technical Report CUED/F-INFENG/TR. 463, Department of Engineering, University of Cambridge.

Khatib O, Sentis L, Park J.H, and Warren J, 2004. Whole-body dynamic behavior and control of human-like robots. International Journal of Humanoid Robotics, 1(1):29-43.

Komura T, Leung H, and Kuffner J, 2004. Animating reactive motions for biped locomotion. In Proc. ACM Symp. onVirtual Reality Software and Technology (VRST 04).

Monnier G, Wang X and Trasbot J, 2008. RPx - A motion simulation tool for automotive interior design. In: Duffy, V. (Ed.), Handbook of Digital Human Modeling: Research for Applied Ergonomics and Human Factors. CRC Press Boca Racon, Florida, USA.

Sardain P and Bessonnet G, 2004. Forces acting on a biped robot. Center of pressure—Zero moment point, IEEE Trans. Syst., Man, Cybern. A, vol. 34, pp. 630 - 637.

Wieber P.B, 2002. On the stability of walking systems. In Proceedings of the Inter-national Workshop on Humanoid and Human Friendly Robotics, 2002.

Zordan V, Majkowska A, Chiu B, and Fast M, 2005. Dynamic response for motion capture animation. Proc. ACM SIGGRAPH 2005 24, 3, 697–701.

Appendix

Appendix 1: Criterion synthesis

If there are n (n≥1) forces of contact: $f = \begin{bmatrix} f_1 \\ \vdots \\ f_n \end{bmatrix}$, for all the points of contact, we must have

$$A_f f \le 0 \qquad (11)$$

with $A_f = diag(\beta_1, \cdots, \beta_n)$.

In order to get the vertices, we need to enclose the polytope by defining another constraint for the vertical force:

$$A_v f = \sum_{i=1}^{n} f_z^i \le f_{limit} \qquad (12)$$

By combining equation (11) and (12), we get:

$$A_c f \le b_c \qquad (13)$$

where $A_c = \begin{bmatrix} A_f \\ A_v \end{bmatrix}$ and $b_c = \begin{bmatrix} 0_{4n,1} \\ f_{limit} \end{bmatrix}$

A grasping force f_i must be constrained by : $\|f_i\| \le f_g^{\max}$

i.e. the force vector must be limited inside a sphere in the $\Re^3$ space. To simplify the problem, we only check this condition along the three axis of the GCS:

$$A_{gi} f_i \le b_{gi} \qquad (14)$$

where $A_{gi} = \begin{pmatrix} 1 & 0 & 0 \\ -1 & 0 & 0 \\ 0 & 1 & 0 \\ 0 & -1 & 0 \\ 0 & 0 & 1 \\ 0 & 0 & -1 \end{pmatrix}$ and $b_{gi} = \begin{bmatrix} f_{gx}^{\max} \\ f_{gx}^{\max} \\ f_{gy}^{\max} \\ f_{gy}^{\max} \\ f_{gz}^{\max} \\ f_{gz}^{\max} \end{bmatrix}$.

If there are k (k≥1) grasping forces $f = \begin{bmatrix} f_1 \\ \vdots \\ f_k \end{bmatrix}$ that have the same force limit, the constraints over the grasping forces:

$$A_g f \le b_g \qquad (15)$$

where $A_g = diag(A_{gi}, \cdots, A_{gi})$ and $b_g = \begin{bmatrix} b_{g1} \\ \vdots \\ b_{gk} \end{bmatrix}$.

We can integrate the n contact forces and the k grasping forces in one vector, then the equations (14) and (15) can be synthesized in one equation :

$$A_{cg} f \le b_{cg} \qquad (16)$$

with

$f = \begin{bmatrix} {}^1 f_c \\ \vdots \\ {}^n f_c \\ {}^1 f_g \\ \vdots \\ {}^k f_g \end{bmatrix}$, $A_{cg} = \begin{bmatrix} A_c & 0 \\ 0 & A_g \end{bmatrix}$ and $b_{cg} = \begin{bmatrix} b_c \\ b_g \end{bmatrix}$.

Appendix 2: Algorithm of polytope computation

Given the polytope *F*, we calculate the polytope ϖ in the following steps:

1. Calculate the vertices $V = \begin{Bmatrix} v_1^t \\ \vdots \\ v_s^t \end{Bmatrix}$ of the polytope *F* from its H-representation;

2. Calculate V_p (the projections of V in the space of $\begin{bmatrix} w \\ \hat{x}w \end{bmatrix}$);

3. Generate the polytope P from V_p and get its H-representation (i.e. $H\begin{bmatrix} w \\ \hat{x}w \end{bmatrix} \le h$);

4. Rewrite the H-representation in function of w and get the H-representation of the new polytope ϖ:

$$\varpi := \left\{ w \in \Re^3 : (H_1 + H_2 \hat{x}) w \le h \right\}.$$

The Algorithm 1 shows how the function *generatePolytope()* calculates the matrix *H1*, *H2* and *h* for each interaction configuration. This algorithm is coded in Matlab and it uses the MPT toolbox (written by Automation Control Laboratory, ETH, Zurich) to carry out the manipulations of polytopes.

Algorithm 1: *generatePolytope()*

Input : *A, C,* A_{cq}, b_{cq}
Output : *H1,H2,h*

1. F = polytope(A_{cg}, b_{cg})

2. V = extreme(F)

3. $P_{ac} = \begin{bmatrix} A \\ C \end{bmatrix}$, $V_p = \begin{Bmatrix} (P_{ac} v_1)^t \\ \vdots \\ (P_{ac} v_s)^t \end{Bmatrix} = \begin{Bmatrix} v_1^t \\ \vdots \\ v_s^t \end{Bmatrix} {P_{ac}}^t = V {P_{ac}}^t$

4. P = hull(V_p,*'extreme_solver'*)

5. [H, h]= double(P)

6. $H_1 = H(:, 1:3)$ and $H_2 = H(:, 4:6)$

Return H1, H2, h